Research article

Functional evaluation of intracranial atherosclerotic stenosis by pressure ratio measurements

Ming Wang [a,1], Xiaochang Leng [b,1], Baojie Mao [c], Rong Zou [b], Dongdong Lin [a], Yuhai Gao [a], Ning Wang [a], Yuning Lu [a], Jens Fiehler [d], Adnan H. Siddiqui [e], Jiong Wu [a], Jianping Xiang [b,**], Shu Wan [a,*]

[a] Brain Center, Zhejiang Hospital, Hangzhou, China
[b] ArteryFlow Technology Co., Ltd., Hangzhou, China
[c] Zhejiang Chinese Medical University, Hangzhou, China
[d] Department of Diagnostic and Interventional Neuroradiology, University Medical Center Hamburg-Eppendorf, Germany
[e] Department of Neurosurgery and Radiology, University at Buffalo, Buffalo, NY, USA

ARTICLE INFO

ABSTRACT

Background: Fractional flow reserve is widely used for the functional evaluation of coronary artery stenosis. Some studies have similarly used the translesional pressure ratio measurements for the functional evaluation of intracranial atherosclerotic stenosis. In this paper, we aimed to investigate the relationship between pressure ratio and cerebral tissue perfusion by MR perfusion imaging and provided a non-invasive method for evaluating the functional significance of intracranial atherosclerotic stenosis.

Methods: A total of 18 consecutive patients with intracranial atherosclerotic stenosis patients including 19 stenotic vessels were recruited. The pressure was measured using a pressure guidewire, the pressure ratio before and after the endovascular intervention was calculated and compared with the severity of diameter stenosis and perfusion-derived MR (the time to maximum tissue residue function (Tmax)). Moreover, the DSA-derived pressure ratio was computed using a novel computational fluid dynamics-based model, termed CFD-PR, and was compared with the actual pressure ratio to assess its diagnostic accuracy.

Results: The pressure ratio increased after percutaneous transluminal angioplasty or stenting, while the correlation between pressure ratio and diameter stenosis was not significant. The pressure ratio was negatively correlated with Tmax (r = −0.73, P < 0.01), and a 95% confidence interval for the cutoff value of pressure ratio = 0.67 (95% confidence interval: 0.58–0.76) was suggested. There was a good correlation (mean = 0.02, Spearman's correlation coefficient r = 0.908, P < 0.001) and agreement (limits of agreement: -0.157 to 0.196, P = 0.954) between CFD-PR and the actual pressure ratio.

Conclusions: This exploratory study indicates the pressure ratio may correlate with the perfusion status. The pressure ratio can be calculated through a non-invasive method using a computational fluid dynamics-based method.

1. Introduction

Stroke is the second leading cause of death and a major cause of disability worldwide, and the most common cause of death in China [1]. Over two-thirds of these patients have ischemic strokes. Intracranial atherosclerotic stenosis (ICAS) is one of the major causes of ischemic stroke, especially in the Asian population, with a proportion of 30–50% [2]. Results from two randomized controlled studies showed that high-risk patients with severe stenosis (70–99%) had a 9–12% annual risk of recurrent stroke [3,4]. The recommended first-line treatment for the prevention of recurrent stroke with ICAS is medical management, including antiplatelet therapy, control of risk factors, and lifestyle adjustment. However, even with aggressive medical treatment, symptomatic ICAS patients with severe stenosis are still at high risk of stroke. Thus, intervention is an important treatment alternative for these patients [5–7]. Some clinical studies have demonstrated the short-term efficacy of endovascular stenting in severe symptomatic ICAS patients, although its efficacy is still controversial [8–10].

The indications for intervention are determined by the extent and severity of anatomical stenosis [11], but these can not accurately reflect the hemodynamic status [12]. Perfusion status is another important reference for intervention. Perfusion-derived MR (the time to maximum tissue residue function (Tmax)) is widely used in defining tissue at risk of infarction in the setting of ischemic stroke. Tmax≥6 s is the threshold for identification of penumbral tissue, and the volume of a penumbra of ≥15 ml has been recognized as the threshold to perform endovascular therapy for ischemic stroke caused by large vessel occlusion [13,14], and the value of which in ICAS is currently being assessed. In patients with anterior circulation ICAS, this threshold has been associated with higher rates of neurological deterioration [15–17], suggesting that aggressive treatment for ICAS patients with Tmax≥6 s may benefit their prognosis. It is urgent to develop an accurate indicator, including hemodynamic parameters and collateral circulation evaluation, to guide endovascular treatment for ICAS.

Fractional flow reserve (FFR) was first proposed by Pijls [18] and has been widely used in the functional assessment of coronary artery stenosis. The coronary FFR is defined as the ratio of maximum blood flow during hyperemia distal to a stenotic lesion to normal maximum flow during hyperemia in the same vessel. Several randomized controlled trials have confirmed that FFR-guided percutaneous coronary intervention (PCI) can effectively improve the prognosis of patients, and FFR≤0.8 was determined as the threshold for intervention [19,20]. Preliminary studies suggested that a similar concept, the translesional pressure ratio (PR) measurements can be applied to cerebral ischemia in ICAS [21–24]. Because the cerebrovascular PR is not the same as the coronary FFR value during hyperemic conditions, it may have weaker correlation with the hemodynamic significance of the lesion. This limitation, as well as the potential complications caused by pressure wire measurement, hindered the popularization of PR in cerebrovascular stenosis.

Computational fluid dynamics (CFD) has been reported to be used to estimate FFR [25–27]. It is used to solve the governing equations of hydromechanics through computer and numerical methods and to simulate and analyze hydromechanical problems [27]. In this study, we measured the actual PR with a pressure wire, analyzed the correlation of PR with the severity of stenosis and perfusion status, and attempted to apply CFD to estimate PR in patients with ICAS.

2. Methods

2.1. Study population

Eighteen consecutive patients with symptomatic ICAS considered as potential candidates for endovascular intervention were recruited between May and September 2021. They received dual aspirin 100 mg and clopidogrel 75 mg for at least 3 days before the intervention. CT scans were performed immediately after the intervention to rule out intracerebral hemorrhage. Then patients were on aspirin 100 mg and clopidogrel 75 mg once daily for at least three months after stenting, and then swiched to aspirin 100 mg alone for at least one year.

All patients underwent diffusion-perfusion MRI analysis, digital subtraction angiography (DSA) and PR measurements. The final decision on endovascular intervention (percutaneous transluminal angioplasty and/or stenting) was based on the patients' symptomatology, anatomical severity of the stenosis, and the perfusion status.

Exclusion criteria included extracranial stenosis, aneurysm proximal to or distal to the stenotic intracranial artery, a possible nonatherosclerotic cause such as atrial fibrillation or arteritis. This study was approved by the Medical Ethics Committee of Zhejiang Hospital and informed consent of the patients was available.

2.2. Intracranial arterial stenosis measurement

The severity of diameter stenosis was calculated in DSA imaging with 3D rotational angiography according to WASID criteria: diameter stenosis = $[(1-(D_{stenosis}/D_{normal}))] \times 100\%$, where $D_{stenosis}$ is the diameter of the artery at the site of the most severe degree of stenosis and D_{normal} is the diameter of the proximal normal artery [11].

2.3. Direct pressure ratio (PR) measurement

Direct PR was measured as described previously [22]. PR was used as a reference for intervention when the degree of stenosis was inconsistent with symptoms or perfusion status. A pressure wire (0.014 inches, PressureWire Certus, St. Jude Medical Inc, USA) was advanced through a 6-Fr guiding catheter to the petrous segment for the ICA system stenosis or the foraminal segment for the vertebral-basilar artery system stenosis, where the mean arterial pressure was measured as Pa. The pressure wire then traversed the stenosis. The mean arterial pressure distal to the stenosis was measured as Pd. PR was calculated as the ratio of Pd to Pa [21] (PR = Pd/Pa). After the percutaneous transluminal angioplasty (PTA) or stenting, PR was re-measured to check the effect of the intervention.

2.4. Perfusion analysis

All patients who underwent diffusion-perfusion MRI were analyzed with RAPID software (iSchemaView, Menlo Park, CA). The time to maximum tissure residue function (Tmax) is a perfusion parameter used in MRI perfusion here, reflecting the time delay between the contrast bolus arriving in the cerebral proximal large arterial circulation and the brain parenchyma [28]. It was analyzed to assess the perfusion status.

2.5. CFD-PR analysis

The software prototype AccuFFicas (ArteryFlow Technology, Hangzhou, China) was used to calculate PR values for the enrolled patients. AccuFFicas was first used for 3D reconstruction of intracranial artery stenosis (Fig. 1A–D) using the DSA DICOM image series. The vessel model was then reconstructed based on the level set segmentation method [29], which is a robust approach and has been applied widely in the area of medical image segmentation [30].Each case had more than 1 million volume elements containing hexahedra (hex) and split-hexahedra (split-hex) elements. The mesh-independence analysis was done for a patient with a diameter stenosis of 80%. Four meshes with different maximum mesh sizes (0.1 mm, 0.16 mm, 0.2 mm and 0.25 mm) were used to calculate CFD-PR. The CFD-PR value changed in the opposite trend to mesh size and became stable when the mesh size decreased to 0.16 mm. Blood was considered as Newtonian fluid without regard to energy equations and gravity. The basic equation governing the flow was the incompressible Navier-Stokes equation and the laminar simulation was carried out in steady-state using the SIMPLE algorithm and in-house solver. The viscosity coefficient of blood was constant, which was 0.0035 Pa•s, and the density was 1056 kg/m^3. The convergence criterion was 0.00001.

The patient-specific mean flow rate of the inlet boundary was calculated by combining DSA images and a 3D model, referring to the TIMI frame count method commonly used in coronary stenosis research [31]. In most cases, the vessel model has only one outlet. Still, when branches connect the stenosis segment, the outlets are modeled as an opening boundary condition with the flow rate proportional to the cube of its diameter [32]. Since PR is calculated from actual blood pressure, the simulated relative pressure field needs to be adjusted equivalently to calibrate the inlet pressure to be consistent with Pa. The description of the CFD method is summarized in *Supplementary Material 1*.

2.6. Statistical analysis

Continuous variables were presented as means ± standard deviation (S.D) and analyzed by the Shapiro-Wilk test. The Wilcoxon Signed Rank Test was used to compare paired data. Categorical variables were presented as percentages. The correlation between the percentage of diameter stenosis, Tmax and PR, and the correlation between PR and CFD-PR were analyzed by the Spearman's correlation test. The Bland-Altman method was used to analyze the agreement of diagnostic results between CFD-PR and PR. Statistical significance was set at $P < 0.05$, and MedCal (MedCalc Software Inc, Belgium) was used for statistical analysis.
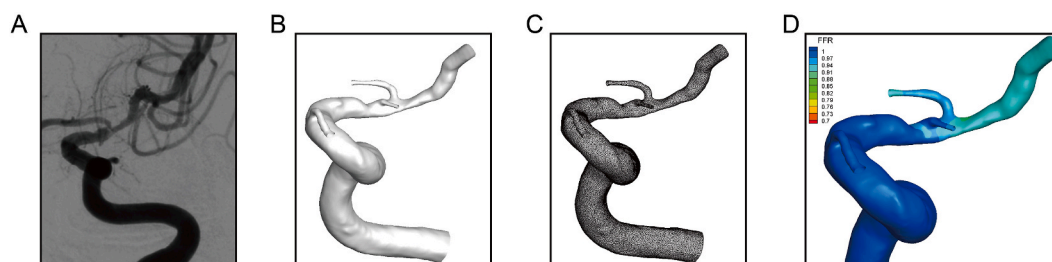

Fig. 1. 3D model reconstruction based on 3D angiography of intracranial arterial stenosis. **A)** DSA image of an intracranial arterial stenosis. **B)** Segmented 3D intracranial arterial stenosis. **C)** Vascular meshing. **D)** Distribution of pressure ratio (PR) results obtained by computational fluid dynamics analysis.

3. Results

3.1. Patient characteristics and pressure measurement

Eighteen patients with 19 intracranial stenotic vessels were included. One patient had artery stenosis both in the right ICA C6 segment and left ICA C7 segment. The mean age was 63.2 ± 11.6 years. There were 12 lesions in the middle cerebral artery M1

Table 1
Patients characteristics and pressure measurement.

NO	Symptom	Site of stenosis	Luminal stenosis (diameter, %)	Status	Pressure wire PP	DP	PR
1	Transient weakness of right hand	L-M1	85	Preoperation	70	25	0.36
				After Stenting	65	47	0.72
2	Weakness of left hand	R–C6	95	Preoperation	79	36	0.46
				After transluminal angioplasty	58	41	0.71
				After Stenting	NA	NA	NA
		L-C7	66	Preoperation	104	79	0.76
				After Stenting	82	68	0.83
3	Weakness of left limb	R-M1	62	Preoperation	79	36	0.46
				After transluminal angioplasty	76	63	0.83
				After Stenting	78	67	0.86
4	Slurred speech	L-M1	66	Preoperation	67	31	0.46
				After transluminal angioplasty	67	42	0.63
				After Stenting	NA	NA	NA
5	Transient weakness of right hand	L-M1	60	Preoperation (without treatment)	80	66	0.83
6	Weakness of right limb	L-M1	68	Preoperation	105	88	0.84
				After Stenting	NA	NA	NA
7	Weakness of left lower limb	R-M1	45	Preoperation	88	47	0.53
				After transluminal angioplasty	83	60	0.72
				After Stenting	83	73	0.88
8	Weakness of left limb	BA	48	Preoperation	86	74	0.86
				After transluminal angioplasty	86	83	0.97
				After Stenting	NA	NA	NA
9	Weakness of left limb	R-M1	76	Preoperation	67	40	0.6
				After transluminal angioplasty	68	58	0.85
				After Stenting	NA	NA	NA
10	Weakness of left lower limb	R–C7	43	Preoperation	76	27	0.36
				After second transluminal angioplasty	63	41	0.65
				After Stenting	57	48	0.84
11	Syncope	L-M1	75	Preoperation	77	34	0.44
				After transluminal angioplasty	88	61	0.69
				After Stenting	NA	NA	NA
12	Weakness of right limb	L-M1	45	Preoperation	29	16	0.55
				After transluminal angioplasty	72	64	0.89
				After Stenting	NA	NA	NA
13	Unsteady walking and dizziness	L-V4	75	Preoperation (without treatment)	94	91	0.97
14	Weakness of left limb	BA	60	Preoperation	87	36	0.41
				After transluminal angioplasty	80	62	0.78
				After Stenting	86	69	0.8
15	Decreased sensation in the right limb	BA	80	Preoperation	52	15	0.29
				After transluminal angioplasty	38	35	0.92
				After Stenting	25	24	0.96
16	Weakness of right limb and slurred speech	L-M1	67	Preoperation	55	32	0.58
				After transluminal angioplasty	57	55	0.96
				After Stenting	NA	NA	NA
17	Lip numbness	R-M1	72	Preoperation	60	19	0.32
				After transluminal angioplasty	57	41	0.72
				After Stenting	58	48	0.83
18	Decreased sensation in the right limb	L-M1	78	Preoperation	72	48	0.67
				After transluminal angioplasty	65	51	0.78
				After Stenting	63	51	0.81

BA: basilar artery, C: internal carotid artery, L: left, M: middle cerebral artery, R: right, V: vertebral artery.

segment (M1), 3 lesions in the intracranial segment of ICA, 3 lesions in the basilar artery and 1 lesion in the vertebral artery V4 segment. Two patients did not receive intervention, as they had mild symptoms, good perfusion status and high PR value. Post-interventinon PR was not measured in 8 patients, as it was difficult for the pressure wire to pass through the stent after the intervention. The symptoms, severity of diameter stenosis, and PR were shown in Table 1. Although the invasive translesional PR measurement with pressure wire is a high-risk operation, it is generally safe. In our study, no hemorrhagic or ischemic complication occurred after the invasive translesional PR measurement in any patients.

3.2. PR increased after the intervention

PR was measured for all 19 vessels before intervention. Only the pre- and post-intervention PR value in treated stenotic arteries were compared in this part, so the PR value were analyzed for 17 vessels before intervention, 14 vessels after percutaneous transluminal angioplasty (PTA) and 9 vessels after stenting. PR increased after PTA and stenting (0.79 ± 0.11 after PTA, 0.84 ± 0.06 after stenting versus 0.53 ± 0.17 pre-intervention; P < 0.01, Fig. 2A).
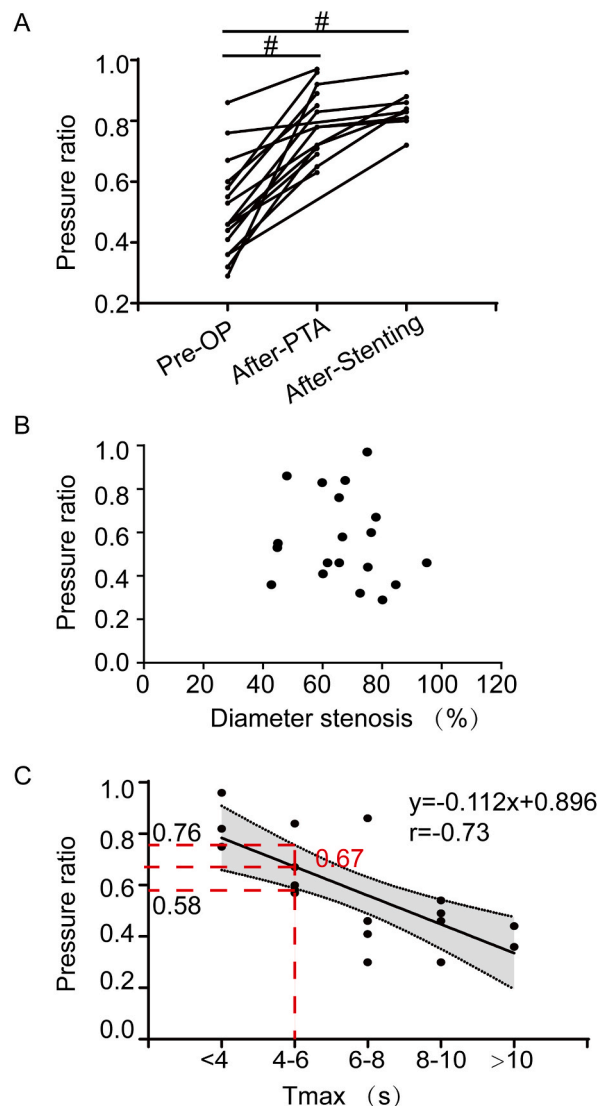

Fig. 2. Clinical application of PR in intracranial arterial stenosis. **A)** Scatterplot showing the value of PR increased from 0.53 ± 0.17 preprocedually to 0.79 ± 0.11 after PTA, and 0.84 ± 0.06 after stenting (P < 0.01). **B)** Scatterplot showing the relationship between PR and diameter stenosis (r = −0.15, P = 0.55). **C)** Scatterplot showing PR was significantly negatively correlated with Tmax (r = −0.73, P < 0.01). When Tmax > 6 s was selected as the intentional indication in our study, we got the cut-off PR value of 0.67 (95% CI: 0.58–0.76).

4. PR was more closely correlated with tmax than with diameter stenosis

PR was more closely correlated with Tmax (r = −0.73, P < 0.01, Fig. 2C) than with diameter stenosis from DSA images (P > 0.05, Fig. 2B). When Tmax≥6 s was selected as the threshold for endovascular therapy in this study, we got the cut-off PR value of 0.67 (95% confidence interval [CI]: 0.58–0.76).

4.1. Correlation and agreement between CFD-PR and PR

Due to incomplete data in some cases, 17 vessels with 27 CFD results in total were included in the analysis. Only 10 vessels had both pre- and post-intervention CFD result, 6 vessels had only pre-intervention results, and 1 vessel had only post-intervention result. CFD-PR values for each lesion were calculated and compared with PR values measured with pressure-wire. Good correlation (Spearman's correlation coefficient r = 0.908, P < 0.0001, 95% CI for r was 0.806–0.958, Fig. 3A) and agreement (limits of agreement: -0.157 to 0.196, P = 0.277, Fig. 3B) were found between CFD-PR and PR.

5. Discussion

Invasively measured coronary FFR has been developed as the gold standard for coronary intervention [33]. Some preliminary studies proved it was feasible to apply a similar concept to evaluate cerebral ischemia in ICAS [21–23]. The cerebrovascular PR resembles the coronary pressure ratio (Pd/Pa) in resting conditions, as intracranial arteries can not reach the level of maximal vasodilation like coronary artery [33]. The hemodynamic correlation of coronary artery stenosis has been studied using an adenosine-free method. The Receiver Operating Characteristic (ROC) analysis showed that the optimal Pd/Pa truncation value with FFR≤0.80 was ≤0.92 (AUC 0.87) [34–37]. Pa/Pd can partially replace the use of FFR to reduce the administration of adenosine, but further confirmation and clinical evaluation in large prospective follow-up studies are required. For intracranial stenosis, instant flow reserve without adenosine infusion can help to identify lesions requiring treatment and prevent the tendency to overtreat a lesion that is not physiologically significant [38].
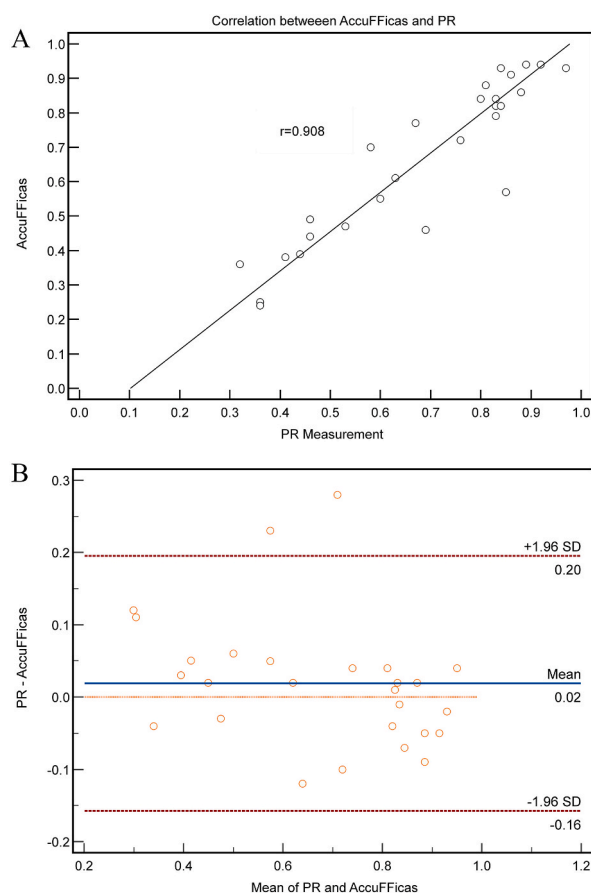

Fig. 3. Good correlation and agreement between CFD-PR and actual PR. A) Correlation between CFD-PR measurement and AccuFFRicas (r = 0.96, p < 0.0001). B) Agreement between CFD-PR measurement and AccuFFRicas values (limits of agreement: -0.151 to 0.149, P = 0.954).

The correlation between the diameter stenosis and PR is currently controversial. Miao et al. analyzed all pre- and post-interventional data from 13 patients and found that PR had a modest correlation ($r = -0.530$, $P = 0.001$) with luminal stenosis. However, the correlation with anterior or posterior circulation lesions was not significant when analyzed separately[21]. While Li et al. demonstrated that a negative correlation was found between PR and diameter stenosis ($r = -0.371$, $P = 0.014$) [39]. In our study, no significant correlation was found between the pre-intervention diameter stenosis and PR. These inconsistent findings suggested that the PR assessment has different manifestations at different sites of lesions. By distinguishing anterior and posterior circulation lesions, or pre-Willisian and post-Willisian lesions, PR may have different correlations with anatomical stenosis of blood vessels.

As previously demonstrated, the coronary FFR was defined as the ratio of maximum blood flow during hyperemia distal to a stenotic lesion to normal maximum flow during hyperemia in the same vessel [40]. Clinically, brain perfusion imaging examination is widely applied to evaluate cerebral collateral blood and compensatory status. Recurrent ischemia is associated with delayed perfusion in ICAS. The early results from the MyRIAD study found no significant association between distal perfusion on PWI (Tmax >4 s, with a volume >5 ml) and recurrent ischemia [23,41]. However, a post hoc analysis of the MyRIAD study defined the abnormal perfusion as Tmax >4 s, with a volume >10 ml, and found the associations with hypoperfusion and border zone infarct pattern, which may be important predictors of early recurrent ischemia in ICAS [23]. Similarly, other studies found anterior circulation ICAS patients with Tmax >6 s had higher rates of neurological deterioration [15–17]. Accordingly, we explored the correlation between PR and Tmax, with Tmax is the abscissa, catergorized by Tmax values (<4s, 4–6s, 6–8s, 8–10s and >10s), and PR as the ordinate. We found a significant negative correlation between them. From the linear correlation, if the value of 6 s for delay on Tmax was taken as the threshold, we could get the cut-off value PR of 0.67 (95% CI: 0.58–0.76). The present study is an exploratory study and more studies are needed to verify the sensitivity and specificity of this cut-off value, and large clinical trials will be performed to confirm its clinical value.

Moreover, we have developed a novel method that allows fast computation of PR from DSA images without pressure wire measurement. In this study, CFD-PR showed a good correlation (Spearman's correlation coefficient $r = 0.908$, $P < 0.001$) and agreement with actual PR. The mean value of the difference between the two methods was 0.00 and the offset was from -0.157 to 0.196, which were acceptable compared with studies on FFR of coronary vessels [42]. Only two points were beyond the range of this interval. Based on the CFD method, PR can be calculated quickly and accurately by reconstructing the intracranial artery stenosis model and using CFD. Intracranial CFD-PR technology combines the advantages of intracranial DSA technology and PR technology to directly calculate the PR values of all blood vessels from the perspective of the DSA image and evaluate the degree of cerebral stenosis from the perspective of vascular structure and function. The advantage of CFD-PR is that it is entirely wire-free and does not require pressure guides or machines. In addition, the application of CFD-PR does not require any change in the existing DSA image acquisition procedure or DSA image acquisition time, nor does it increase the amount of radiation received by patients.

There are several limitations of the present study. The readers should bear in mind the exploratory nature of this study, with some limitations. A multi-centered study with high efficiency is needed to validate PR and the cut-off value. Patients with anterior or posterior circulation lesions were all enrolled in this study, which may lead to statistical bias. So we conducted a subgroup analysis that included M1 stenosis only and found a similar trend as our previous results (*Supplementary Material 2*). Even though, it is still necessary to analyze differently anterior and posterior circulation lesions separately, especially pre-Willisian and post-Willisian lesions, for their different collateral flow. Follow-up data is required to evaluate the clinical value of the usage of PR to guide ICAS treatment. Some patients received diffusion-perfusion MRI at the 6-month follow-up in this study, and we found Tmax decreased in most patients after intervention (Supplementary Material 2). The sensitivity and specificity of PR should be evaluated, and a non-invasive approach, such as CT-derived CFD-PR should be explored in further studies.

6. Conclusion

In summary, this exploratory study demonstrated that PR was more closely related to perfusion status than diameter stenosis in ICAS. CFD-PR showed a good correlation and agreement with pressure wire-measured PR in our study with a limited number of patients. The utility of PR and CFD-PR in evaluation of ICAS requires further studies.

Declarations

Author contribution statement

Funding statement

Data availability statement

Data included in article/supp. Material/referenced in article.

Declaration of competing interest

The authors declare that they have no known competing financial interests or personal relationships that could have appeared to influence the work reported in this paper.

Appendix A. Supplementary data

Supplementary data to this article can be found online at https://doi.org/10.1016/j.heliyon.2023.e13527.

References

[1] S. Wu, et al., Stroke in China: advances and challenges in epidemiology, prevention, and management, Lancet Neurol. 18 (4) (2019) 394–405, https://doi.org/10.1016/S1474-4422(18)30500-3.

[2] J. Koo, The latest information on intracranial atherosclerosis: diagnosis and treatment, Interv Neurol 4 (1–2) (2015) 48–50, https://doi.org/10.1159/000438779.

[3] M.I. Chimowitz, et al., Stenting versus aggressive medical therapy for intracranial arterial stenosis, N. Engl. J. Med. 365 (11) (2011) 993–1003, https://doi.org/10.1056/NEJMoa1105335.

[4] O.O. Zaidat, et al., Effect of a balloon-expandable intracranial stent vs medical therapy on risk of stroke in patients with symptomatic intracranial stenosis: the VISSIT randomized clinical trial, JAMA 313 (12) (2015) 1240–1248, https://doi.org/10.1001/jama.2015.1693.

[5] M.H. Mohammaden, et al., Safety and efficacy of balloon-mounted stent in the treatment of symptomatic intracranial atherosclerotic disease: a multicenter experience, J. Neurointerventional Surg. (2021), https://doi.org/10.1136/neurintsurg-2021-017818.

[6] L. Meyer, et al., Stenting with Acclino (flex) for symptomatic intracranial stenosis as secondary stroke prevention, J. Neurointerventional Surg. 12 (11) (2020) 1127–1131, https://doi.org/10.1136/neurintsurg-2019-015744.

[7] M.J. Alexander, et al., WEAVE trial: final results in 152 on-label patients, Stroke 50 (4) (2019) 889–894, https://doi.org/10.1161/STROKEAHA.118.023996.

[8] Z. Miao, et al., Thirty-day outcome of a multicenter registry study of stenting for symptomatic intracranial artery stenosis in China, Stroke 46 (10) (2015) 2822–2829, https://doi.org/10.1161/STROKEAHA.115.010549.

[9] P. Gao, et al., Multicenter prospective trial of stent placement in patients with symptomatic high-grade intracranial stenosis, AJNR Am J Neuroradiol 37 (7) (2016) 1275–1280, https://doi.org/10.3174/ajnr.A4698.

[10] G. Duan, et al., Solitaire stents for the treatment of complex symptomatic intracranial stenosis after antithrombotic failure: safety and efficacy evaluation, J. Neurointerventional Surg. 8 (7) (2016) 680–684, https://doi.org/10.1136/neurintsurg-2015-011734.

[11] O.B. Samuels, et al., A standardized method for measuring intracranial arterial stenosis, AJNR Am J Neuroradiol 21 (4) (2000) 643–646.

[12] D.S. Liebeskind, et al., Collateral circulation and hemodynamics of severe intracranial atherosclerosis: angiography and clinical correlates at baseline in the SAMMPRIS trial, Stroke 43 (2012) suppl_1.

[13] G.W. Albers, et al., Thrombectomy for stroke at 6 to 16 hours with selection by perfusion imaging, N. Engl. J. Med. 378 (8) (2018) 708–718, https://doi.org/10.1056/NEJMoa1713973.

[14] B.C. Campbell, et al., Endovascular therapy for ischemic stroke with perfusion-imaging selection, N. Engl. J. Med. 372 (11) (2015) 1009–1018, https://doi.org/10.1056/NEJMoa1414792.

[15] A. de Havenon, et al., Hypoperfusion distal to anterior circulation intracranial atherosclerosis is associated with recurrent stroke, J. Neuroimaging 30 (4) (2020) 468–470, https://doi.org/10.1111/jon.12710.

[16] S. Yaghi, et al., What threshold defines penumbral brain tissue in patients with symptomatic anterior circulation intracranial stenosis: an exploratory analysis, J. Neuroimaging 29 (2) (2019) 203–205, https://doi.org/10.1111/jon.12577.

[17] K. Dakay, S. Yaghi, Symptomatic intracranial atherosclerosis with impaired distal perfusion: a case study, Stroke 49 (1) (2018) e10–e13, https://doi.org/10.1161/STROKEAHA.117.019173.

[18] N.H. Pijls, et al., Experimental basis of determining maximum coronary, myocardial, and collateral blood flow by pressure measurements for assessing functional stenosis severity before and after percutaneous transluminal coronary angioplasty, Circulation 87 (4) (1993) 1354–1367, https://doi.org/10.1161/01.cir.87.4.1354.

[19] B. De Bruyne, et al., Fractional flow reserve-guided PCI versus medical therapy in stable coronary disease, N. Engl. J. Med. 367 (11) (2012) 991–1001, https://doi.org/10.1056/NEJMoa1205361.

[20] P. Xaplanteris, et al., Five-year outcomes with PCI guided by fractional flow reserve, N. Engl. J. Med. 379 (3) (2018) 250–259, https://doi.org/10.1056/NEJMoa1803538.

[21] Z. Miao, et al., Fractional flow assessment for the evaluation of intracranial atherosclerosis: a feasibility study, Interv Neurol 5 (1–2) (2016) 65–75, https://doi.org/10.1159/000444333.

[22] Y.F. Han, et al., Severity assessment of intracranial large artery stenosis by pressure gradient measurements: a feasibility study, Cathet. Cardiovasc. Interv. 88 (2) (2016) 255–261, https://doi.org/10.1002/ccd.26414.

[23] S. Prabhakaran, et al., Predictors of early infarct recurrence in patients with symptomatic intracranial atherosclerotic disease, Stroke 52 (6) (2021) 1961–1966, https://doi.org/10.1161/STROKEAHA.120.032676.

[24] M. Wang, et al., Cerebral Fractional Flow Reserve for Functional Evaluation of Intracranial Atherosclerotic Stenosis, Transl Stroke Res, 2022, https://doi.org/10.1007/s12975-022-01034-3. Epub 20220530.

[25] J. Liu, et al., Functional assessment of cerebral artery stenosis: a pilot study based on computational fluid dynamics, J. Cerebr. Blood Flow Metabol. 37 (7) (2017) 2567–2576, https://doi.org/10.1177/0271678X16671321.

[26] C.A. Taylor, T.A. Fonte, J.K. Min, Computational fluid dynamics applied to cardiac computed tomography for noninvasive quantification of fractional flow reserve: scientific basis, J. Am. Coll. Cardiol. 61 (22) (2013) 2233–2241, https://doi.org/10.1016/j.jacc.2012.11.083.

[27] W. Jiang, et al., Diagnostic accuracy of coronary computed tomography angiography-derived fractional flow reserve, Biomed. Eng. Online 20 (1) (2021) 77, https://doi.org/10.1186/s12938-021-00914-3.

[28] A. Wouters, et al., A comparison of relative time to peak and Tmax for mismatch-based patient selection, Front. Neurol. 8 (2017) 539, https://doi.org/10.3389/fneur.2017.00539.

[29] L. Antiga, et al., An image-based modeling framework for patient-specific computational hemodynamics, Med. Biol. Eng. Comput. 46 (11) (2008) 1097–1112, https://doi.org/10.1007/s11517-008-0420-1.

[30] X. Tong, et al., Predicting flow diverter sizing using the AneuGuide(TM) software: a validation study, J. Neurointerventional Surg. (2022), https://doi.org/10.1136/neurintsurg-2021-018353. Epub 2022/01/19.

[31] C.M. Gibson, et al., TIMI frame count: a quantitative method of assessing coronary artery flow, Circulation 93 (5) (1996) 879–888, https://doi.org/10.1161/01.cir.93.5.879.

[32] C.D. Murray, The physiological principle of minimum work applied to the angle of branching of arteries, J. Gen. Physiol. 9 (6) (1926) 835–841.

[33] B. De Bruyne, et al., Relation between myocardial fractional flow reserve calculated from coronary pressure measurements and exercise-induced myocardial ischemia, Circulation 92 (1) (1995) 39–46, https://doi.org/10.1161/01.cir.92.1.39.

[34] A. Hakeem, et al., Derivation and validation of Pd/Pa in the assessment of residual ischemia post-intervention: a prospective all-comer registry, Cathet. Cardiovasc. Interv. 99 (3) (2022) 714–722, https://doi.org/10.1002/ccd.29790.

[35] G. De Luca, et al., Resting Pd/Pa and haemodynamic relevance of coronary stenosis as evaluated by fractional flow reserve, Coron. Artery Dis. 29 (2) (2018) 138–144, https://doi.org/10.1097/MCA.0000000000000561.

[36] C.K.M. Boerhout, et al., Combined use of hyperemic and non-hyperemic pressure ratios for revascularization decision-making: from the ILIAS registry, Int. J. Cardiol. (2022), https://doi.org/10.1016/j.ijcard.2022.11.015. Epub 2022/11/14.

[37] Z. Piroth, et al., Correlation and relative prognostic value of fractional flow reserve and Pd/Pa of nonculprit lesions in ST-segment-elevation myocardial infarction, Circ Cardiovasc Interv 15 (2) (2022) e010796, https://doi.org/10.1161/CIRCINTERVENTIONS.121.010796.

[38] R.H. Dossani, et al., Measurement of instant flow reserve to quantify functional flow limitation across stenosis in intracranial atherosclerotic disease, J. Neurointerventional Surg. 12 (12) (2020) 1248, https://doi.org/10.1136/neurintsurg-2020-016080.

[39] L. Li, et al., Hemodynamic versus anatomic assessment of symptomatic atherosclerotic middle cerebral artery stenosis: the relationship between pressure wire translesional gradient and angiographic lesion geometry, Front. Neurol. 12 (2021), 671778, https://doi.org/10.3389/fneur.2021.671778.

[40] N.H. Pijls, et al., Fractional flow reserve versus angiography for guiding percutaneous coronary intervention in patients with multivessel coronary artery disease: 2-year follow-up of the FAME (Fractional Flow Reserve versus Angiography for Multivessel Evaluation) study, J. Am. Coll. Cardiol. 56 (3) (2010) 177–184, https://doi.org/10.1016/j.jacc.2010.04.012.

[41] J.G. Romano, et al., Infarct recurrence in intracranial atherosclerosis: results from the MyRIAD study, J. Stroke Cerebrovasc. Dis. 30 (2) (2021), 105504, https://doi.org/10.1016/j.jstrokecerebrovasdis.2020.105504.

[42] C. Li, et al., Diagnostic performance of angiography-based fractional flow reserve for functional evaluation of coronary artery stenosis, Front Cardiovasc Med 8 (2021), 714077, https://doi.org/10.3389/fcvm.2021.714077.